SATEG CORP

Final Project Report

Department of Applied Ocean Physics & Engineering

Woods Hole Oceanographic Institution (WHOI)

Contact:

Amanda Besaw (abesaw@whoi.edu)

WHOI Purchase Order: E122375

Project Title:

Experimental Study of a Scalable Arctic Thermoelectric Generator (SATEG) for Low-Power Arctic Sensors and Data Transmission, Scalable for AUV Charging

Principle Investigator: Dr. Yuriy Lobunets

Project Performance Period: March – June 2021

SATEG CORP

771 Elmgrove Rd

Rochester, NY 14624

James Galloway (james.galloway@sategcorp.com)

Executive Summary

The purpose of this project was to demonstrate the working principles and experimentally verify the mathematical modeling data of a Scalable Arctic Thermoelectric Generator (SATEG) capable of meeting target operating requirements (previously defined in ONR project N6833520C05). The SATEG uses thermoelectrics to generate electricity from the energy potential between the Arctic Ocean/air temperature differences. The main challenge of this form of energy harvesting is that temperature differences are small and dispersed over a large area. During the year, the air temperature fluctuates in a fairly wide range (from -52°C to +32°C), while water temperature is almost constant (from -2°C to +3°C). The difference between water and air temperatures is the energy potential that can be used to convert into electricity.

In support of the project objectives, two different SATEG laboratory prototype units were designed, fabricated, and tested in simulated environments. The results were compared with the theoretical model and demonstrated excellent conformity. The parameters of the studied SATEG modules corresponded to the power parameters of an ice buoy with an average power consumption of 8W. The experience obtained from the fabrication and testing of the two SATEG prototypes further enhanced the understanding of practical design issues, which will form the basis of follow-on research toward the design of a field-deployable SATEG device and toward its eventual commercialization.

Work Performed & Technical Discussion

Background

The energy conversion system for the SATEG is the thermoelectric method of direct conversion of thermal energy into electricity. It is based on the Seebeck effect, which consists of the appearance of an EMF during the heat flow in a circuit consisting of dissimilar materials. The basic building-block of a thermoelectric generator (TEG) contains semiconductor elements of p- and n-type connected in series, as shown in Figure 1. These individual elements and their electrical interconnects are mounted between two ceramic plates. The plates hold the overall structure together mechanically and electrically insulate the individual elements from one another and from external surfaces. The temperature difference between the junctions of elements creates the EMF (*E)*, proportional to the temperature difference on the elements $\Delta T=(T_h-T_c)$:

$$E=en_v\Delta T \qquad (1)$$

here e is the Seebeck coefficient; n_v – the number of elements; T_h and T_c – the junction temperatures of the elements.

Figure 1. Thermoelectric Module

If the circuit is completed with a load (R_L), an electric current is generated:

$$I=E/(R+R_L), \qquad (2)$$

here $R= n_v h/\sigma s$ – electrical resistance of the thermoelectric module; h – leg lengths; σ – electrical conductivity coefficient; s – cross-sectional area of the leg.
Therefore, useful power N is generated:

$$N = \frac{E^2}{R}\,\frac{m}{(m+1)^2}\,, \qquad (3)$$

where $m = R_L/R$ – load factor.

<u>Conceptual Design of the SATEG</u>

The concentration of heat flows for effective transfer of thermal energy between the heat source and heat sink through a TEG is a critical aspect of the SATEG design. The selected technical approach to this problem is the use of a two-phase heat exchange system, known as a closed thermosyphon. The thermosyphon is a sealed, pre-evacuated chamber (typically in the form of a pipe) with a fixed amount of working fluid inside. Under isothermal conditions, the saturated vapor pressure of the liquid phase is constant inside the chamber. When the upper part of the pipe is cooled, the vapor begins to condense, a pressure gradient forms, and vapor flows from the lower to the upper part of the pipe. The condensate flowing down under gravitational force feeds into the evaporation zone, completing the closed heat transfer circuit. This passive heat exchange mechanism transfers heat from the lower part to the upper part of the pipe without forced circulation.

The SATEG design consists of two separate heat exchanger thermosyphons, each of which has a ribbed tubular heat exchanger and an evaporator/condenser chamber in the form of a rectangular plate. A set of thermoelectric modules that make up the TEG is located between the chambers. The power of SATEG is determined by the size of its components and the ratio of thermal resistances of the water heat exchanger Rw, air heat exchanger Ra and TEG Rg. The theory of calculation and optimization of such devices is set out in detail by the PI's in an article published earlier this year[1] (attached hereto as Appendix III).

Thermosyphon Design

Two thermosyphon geometries were fabricated, one with threaded and the other with welded connections. While welded connections are more reliable and should be incorporated into the field-deployable device, the threaded design is more convenient for lab testing, making modifications in the lab, and for transporting the device. The basic thermosyphons design developed for the SATEG is shown in Figure 2. Additionally, two geometries for the evaporator chamber of the thermosyphon with different configuration of the internal flow channels were designed, fabricated and evaluated (Figure 3). Since the thermal resistance of any heat exchanger is inversely proportional to the product of the coefficient of heat transfer and its surface area, the configuration of the evaporation chamber is selected based on maximum surface area, limited by mechanical design constraints. The other limiting factor is the area of the surface contact between the chamber and the thermoelectric modules. Based on these design constraints, a micro-channel design is an ideal heat exchange configuration for the SATEG, because the coefficient of heat transfer per unit of surface area is significantly higher than in a conventional design, while assuring mechanical robustness of the design. Based on preliminary analysis, this will reduce the mass of the evaporation chambers 3-4 fold.

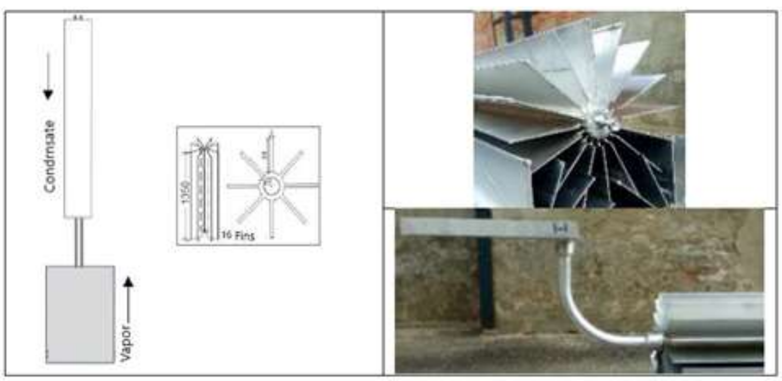

Figure 2. Heat Exchanger Thermosyphon SATEG Module

[1] Yuriy Lobunets. *Improving the Economic Efficiency of Thermoelectric Generators by Optimizing Heat Transfer Conditions.* - Journal of Electronics Materials, 2021. DOI:10.1007/s11664-021-08797-9.

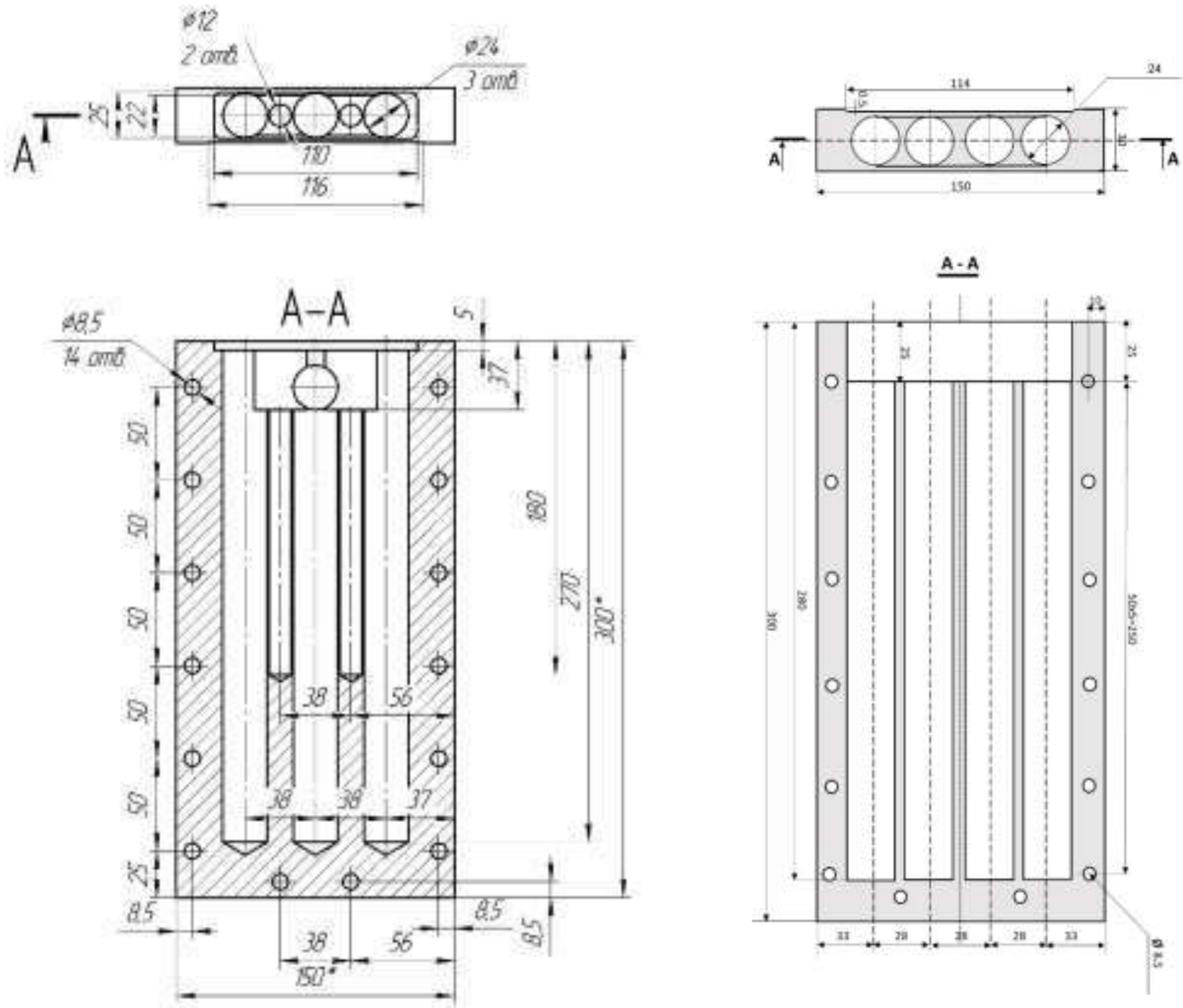

Figure 3. Two Vapor Chamber Designs

Heat-carrier Selection

Theoretically, the heat carrier inside the thermosyphons may be any chemical that has both liquid and gaseous phases in the operating temperature range (-52°C to +32°C). Additionally, the selected heat-carrier should have the following properties:

- high latent heat of vaporization;
- high coefficient of surface tension;
- good wetting properties with respect to the structural material of the thermosyphons;
- high vapor density in the operating temperature range and low density in the liquid phase;
- vapor pressure at saturation should be low to provide for thin heat exchanger walls and safe operating conditions;

- critical parameters of the heat-carrier should be significantly higher than the working parameters, because an increase in temperature leads to a decrease in surface tension and heat of vaporization decrease and becomes zero at the critical point;
- compatible with the structural materials of the thermosyphons, across the temperature range (i.e. does not cause corrosion);
- environmentally safe.

The thermophysical characteristics of six SATEG thermosyphons assemblies with two different design geometries of the heat-carrier chamber and different chemistries (i.e. pentane, isobutane, and freon R410A) were experimentally studied. Any of these heat carriers can be used in a specified temperature range (their properties are given in Appendix II). Ammonia, as originally proposed, was not used during the laboratory testing out of practical safety concerns. To determine the advantages and disadvantages of each heat carrier, it is necessary to conduct more detailed research.

Testing

The main purpose of the study was to determine the characteristics of heat transfer (thermal resistance) within the SATEG module, which determines the technical parameters of the device, in order to corroborate the previously modeled performance data. Specifically, the main working characteristic of a SATEG module is the dependence of thermal resistance *Rt* on the temperature difference between water t_w and air t_a. Figures 4 - 5 presents the experimental setup for *Rt* studies and measurement results. This part of the research concerned only the determination of the thermal resistance of the thermosyphons (i.e. the boiling and condensation processes). Measurement of heat fluxes Q were carried out and the temperature fields of the thermosyphons were investigated. Table 1 shows an example of test results.

Table 1. Test Results for Thermosyphon Testing

Q, W	T1	T2	T3	T4	T5	T6	T7	Rt, K/W
100	14.7	14.2	9.7	9.8	10.1	9.4	11.9	0.040
200	17.7	17.3	12.3	12.2	12.4	11.8	12.5	0.026
300	21.3	20.9	16.2	16.2	15.9	15.2	15.5	0.019
400	26.4	26.0	21.9	21.9	21.0	20.2	20.6	0.014
500	32.5	32.3	28.8	28.8	26.8	27.3	27.3	0.011
600	42.6	42.4	39.9	39.9	36.6	38.2	38.3	0.008

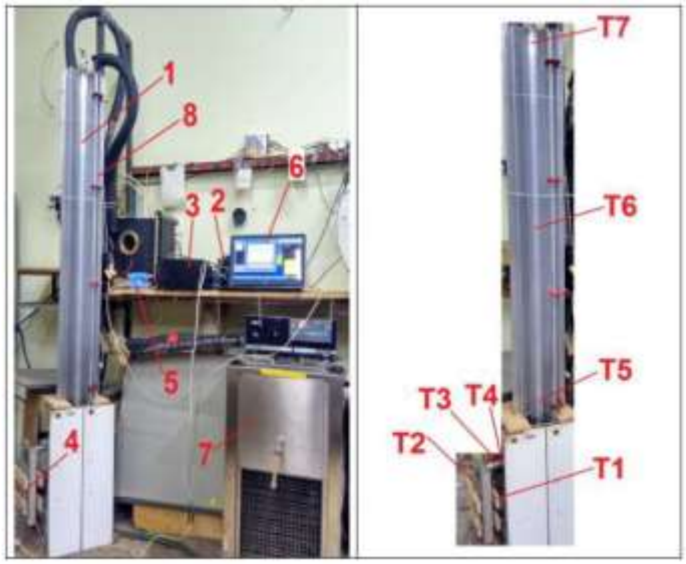

Figure 4. Test Rig (left) and Measurement Thermocouple Locations (right)

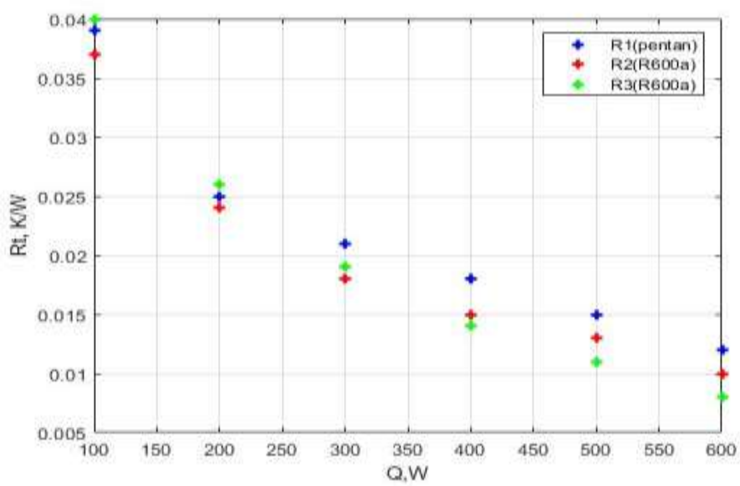

Figure 5. Thermal Resistance of a Thermosyphon vs Heat Power

To evaluate the efficiency of the air heat exchanger and control the parameters, the cooling rate of a fixed volume of water was measured. The corresponding experimental data are presented in Figure 6. These results confirmed the selected range of heat transfer intensity for the calculations of the air heat exchanger (it is 5 - 10 W/m^2K).

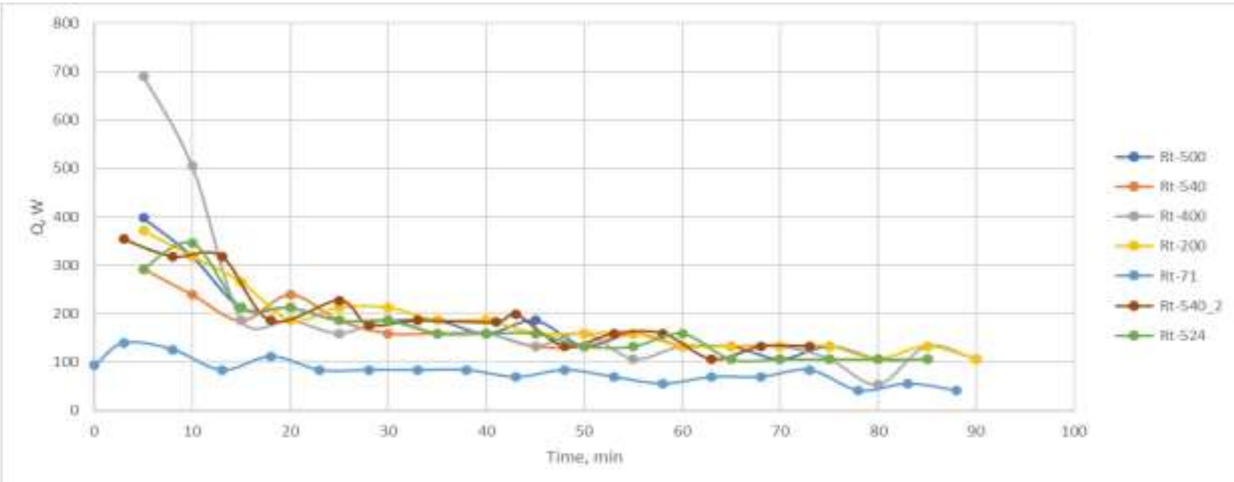

Figure 6. Cooling Rate of Thermosyphon with Different Volumes of Heat-carrier

The next phase of the research was the SATEG test assembly, comprised of two thermosyphons and a series of TEG's, as shown in Figure 7.

Figure 7. SATEG Module (left) and SATEG Module Inside Test Apparatus (right)

The water heat exchanger was located in a tank with water or in a natural pond (i.e. it worked in conditions close to full-scale; Figures 8 - 9). To ensure low air temperatures, the air heat exchanger was chilled by liquefied nitrogen. These conditions do not completely model actual Arctic conditions, so the determining factor was the temperature of the condensate in the air thermosyphon t_{ca}. The dependences of SATEG EMF on the temperature difference and the corresponding dependences of SATEG power are shown in Figures 10 - 11. These data represent several series of tests in different conditions. Some scattering of the data is due to measurement errors that are within acceptable limits for a thermophysical experiment.

Figure 8. Lab Test Rig.

Figure 9. Field Test Rig

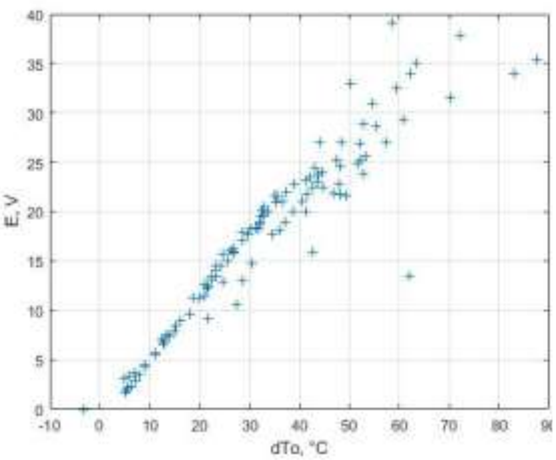

Figure 10. Experimental Data E=f(dTo).

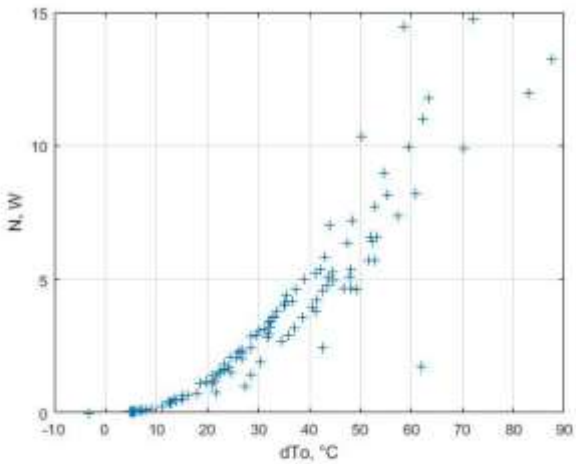

Figure 11. Experimental Data N=f(dTo)

A clearer correlation is given by the results in which the EMF of the SATEG was used to determine the temperature difference (Figures 12 - 13). In this case, the TEG is considered as a highly sensitive and high-precision temperature sensor, which provides the average value of the temperature difference.

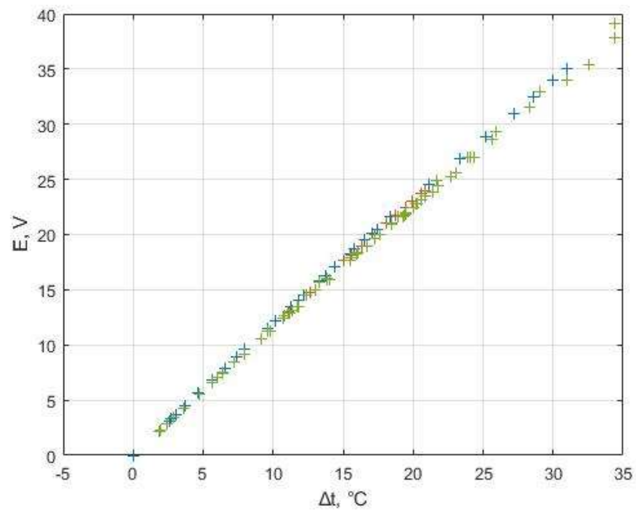

Figure 12. Experimental Data E=f(Δt).

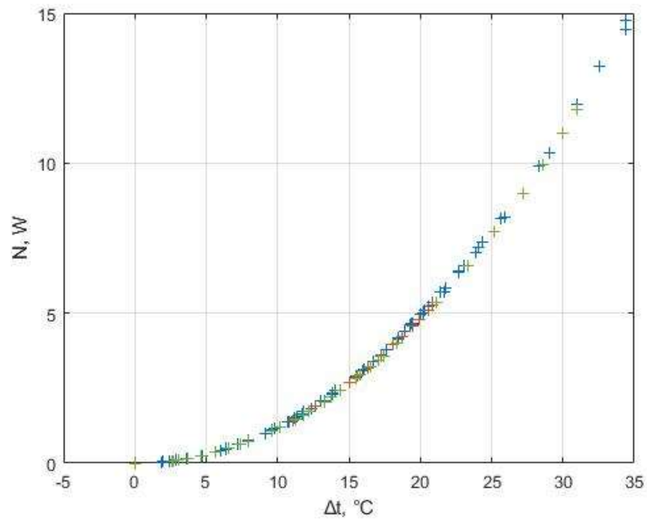

Figure 13. Experimental Data N=f(Δt)

A comparison of experimental (markers) and calculated (curves) data is shown in Figures 14 - 15. These results are in excellent agreement with the results of the mathematical model.

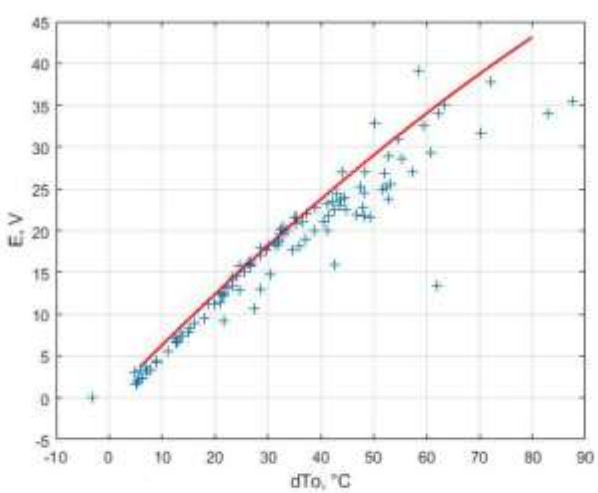

Figure 14 E=f(dTo)

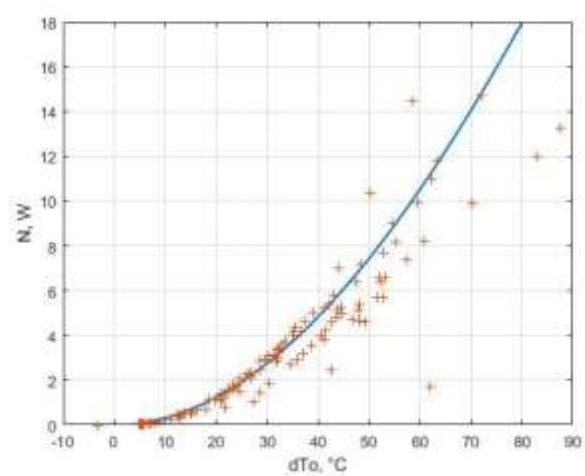

Figure 15. N=f(dTo)

Design Lessons Learned

The fabrication and testing of the first generation SATEG prototype modules has resulted in several practical lessons that will be incorporated into subsequent generation designs:

- Multiple air-side thermosyphons paired with a single water-side thermosyphon create unnecessary fabrication complexity;
- Welded connections offer added reliability;
- TEG unit should be pre-assembled and vacuum packed into a single component;
- Large surface-area collector chamber without reinforcement ribs inside the evaporator has potential for ballooning from internal pressure.

Conclusions

The completed experimental research has shown an excellent correlation of test and calculated data for the characteristics of the proposed concept for an Arctic Ocean heat energy converter. This supports the viability of the SATEG, having such favorable features as passive design without moving mechanical parts, modularity, scalability, and low cost. Under the defined conditions of use, its operating lifetime is not limited by anything (i.e. SATEG is able to provide electricity to Arctic missions for an indefinite time period), excluding catastrophic events such as curious polar bears or shifting icebergs. Furthermore, this approach to energy harvesting / scavenging has potential applications beyond the water-air Arctic environment and in conditions of glacier-air or soil-air, which opens up additional potential fields of use in the Arctic and Antarctica theaters.

Recommendations

To further develop the SATEG, it is necessary to conduct research and development of improved designs using advanced microchannel heat transfer systems and/or 3D printing technologies. For the next iteration of the SATEG (second generation), the following design approach is recommended which does not require significant research and is based on off-the-shelf materials:

- Replace machined evaporator plates with micro-channel extrusions;
- Incorporate pre-assembled vacuum packed TEG;
- Select heat carrier with low vapor pressure (<7 atm) at highest possible operating temperature (+32°C).

At the next stage of research, it is necessary to conduct experimental operation of a SATEG in real-world conditions with constant monitoring of meteorological data and the corresponding energy characteristics of the generator. The design, which incorporates the above changes, can be fabricated within 3 - 4 months for testing in a practical simulated “Arctic” environment such as an accessible frozen lake during the 2021 – 2022 winter season.

APPENDIX I

1. **Characteristics of the thermoelectric module**

Type	MT2,4-0,13-299
thermoelectric material	Bi_2Te_3
size	52x56 mm
number of thermocouples	299
height of thermocouples	1.3 mm
cross section of the thermocouple	2.4 mm^2

2. **Thermoelectric properties**

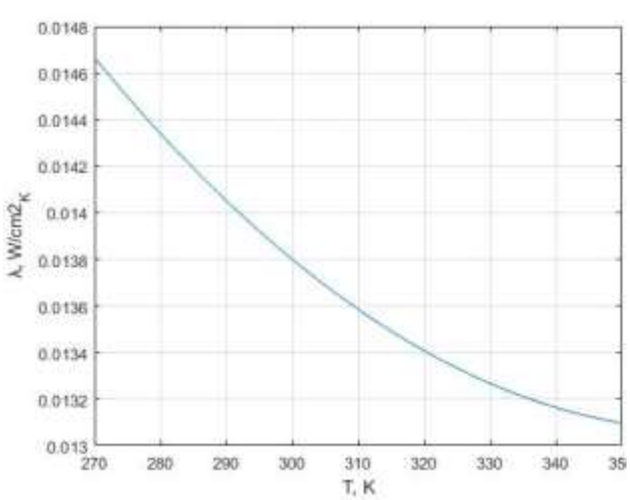

Thermal conductivity

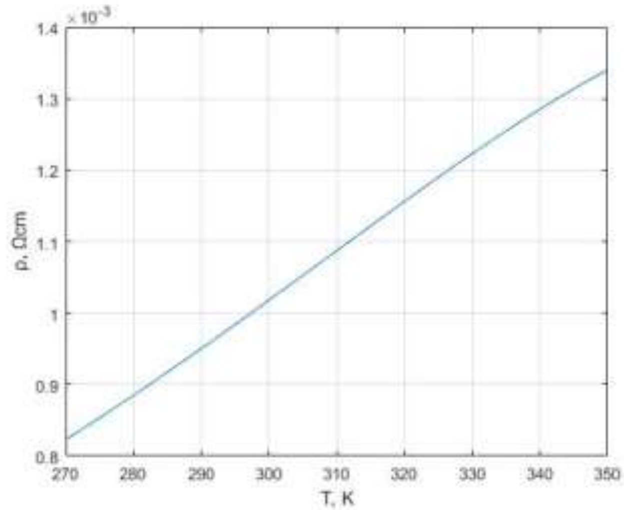

Electrical conductivity

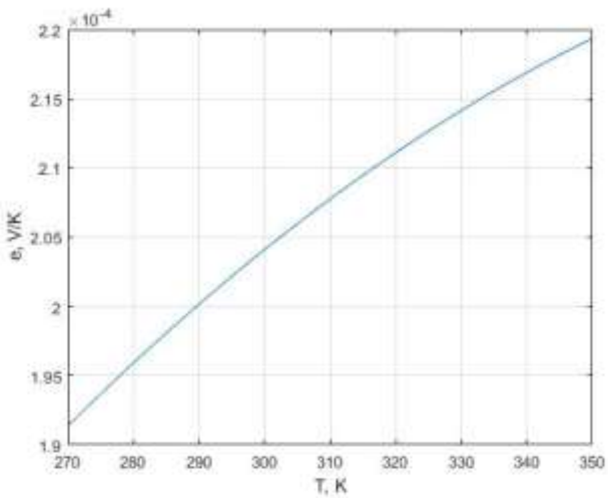

Seebeck coefficient

APPENDIX II

Properties of heat carriers.

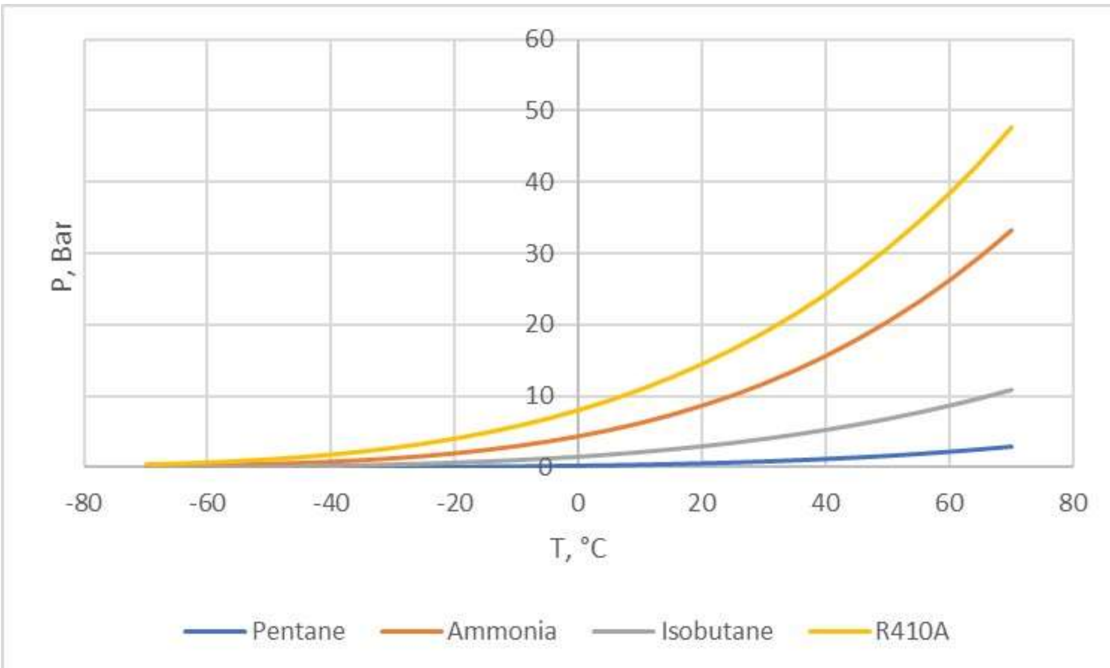

APPENIDX III

Yuriy Lobunets. *Improving the Economic Efficiency of Thermoelectric Generators by Optimizing Heat Transfer Conditions.* - Journal of Electronics Materials, 2021. DOI:10.1007/s11664-021-08797-9.